Supplementary material for:

Threats from the air: damselfly predation on diverse prey taxa

Kaunisto K. M., Roslin T., Forbes M., Morrill A., Sääksjärvi I. E., Puisto A. I. E., Lilley T. M. & Vesterinen E. J.

Journal of Animal Ecology

correspondence to: kkauni@utu.fi

This supplementary material includes:

Detailed materials and methods

Here we offer full details of the methods applied, starting from the summary text from the main document but adding more detailed protocols and bioinformatics.

Sampling and study site

To assess the population sizes and survival rates of the focal species, we conducted a Mark-Release-Recapture (MRR) study of the damselfly populations associated with a freshwater pond of

approximately 600 m x 200 m (12 ha). This pond is surrounded by meadows in a suburban landscape. To compare prey use among the focal species against the background of the pool of prey available to those species, all samples of predators were collected 5–8 m from the water body along a straight path of *ca.* 85 m. This census route was sampled 14 times between 31 May - 1 August, 2016. Individuals were captured with a sweep net, identified to species and sex, and marked with dark, non-toxic permanent pen on their hind wings. After marking, individuals were released and recaptured when encountered.

During the MRR study on 1 June and 2 June, we collected an additional 185 individuals (20–26 males and females from each species) for faecal DNA analysis. Each individual was placed into a 'clean' 10-ml collection tube housing a piece of dampened paper towel to avoid desiccation. To allow complete defecation, damselflies were kept in the tubes for the next 24 h (complete defecation time according to Higashi 1973, Fried and May 1983, Kaunisto et al. 2017). All the faecal material was collected from the tubes, after which the faeces were frozen in 15 ml Falcon tubes at – 64° C until further analysis.

Prey populations were sampled using nine special emergence traps (Figure S1) designed by EJV in an earlier study (Lilley et al. 2012).

Figure S1. An emergence trap used to catch developing insects on the water surface. The trap was constructed from eight 1 meter long plastic pipes that were joined together to form a 1x1 meter bottom and a pyramid-like frame, where the mesh was attached. The top-end of the mesh was connected to an ethanol-filled collection bottle, where the emerging insects ended up. For details, see Lilley et al. (2012).

MRR estimates

Damselfly abundances and all other population estimates were modeled using MARK software (version 9.0; Cooch and White 2018). We applied Jolly-Seber methods under the POPAN parameterization (Lebreton et al. 1992) to our mark-release-recapture data. This particular application of Jolly-Seber methods is suitable for open populations and assumes that all individuals have equal probability of capture (p) at each specific sampling occasion, and that all individuals have the same probability of survival (ϕ) during each separate interval between sampling occasions. This formulation also considers (and estimates) probabilities of new individuals entering the population (*pent*) between sampling points, and in addition to these three primary parameters (p, ϕ, and *pent*) calculates several derived parameters: abundance estimates at each sampling occasion

(N_t) and the overall population size (N_{Tot}), or superpopulation, referring to the total number of individuals present across all sampling occasions included.

MARK software calculates primary population parameters through maximum likelihood estimation and allows comparison of models wherein these parameters may vary with time either in a factorial (t), linear (T), or polynomial (T^2) manner, or as constant within the model (indicated by (.); time-independency). Given the consistent sampling methodology and unchanging sampling locale, and as all damselfly species emergence rates are known to vary over the span of time during which this study took place, we fit models wherein the probability of individuals entering the population was always time-dependent ($pent_{(t)}$, $pent_{(T)}$, or $pent_{(T2)}$), where survival was either constant or time-dependent ($\phi_{(.)}$, $\phi_{(t)}$, $\phi_{(T)}$, or $\phi_{(T2)}$), and capture probability was kept constant ($p_{(.)}$), to maintain biological realism. Models were compared using the Akaike's Information Criterion corrected for small sample sizes, AICc (Burnham and Anderson 2002): the lowest-scoring models were considered to provide the best fit, and models with AICc scores differing by less than two from the lowest-scoring candidate were considered equivalent (Burnham and Anderson 2002).

Average longevity of damselflies within each of the four sampled populations was calculated using the model-estimated survival (ϕ) estimates, averaged across all daily values (ϕ') when time-dependent, using the formula $-\ln(\phi')^{-1}$ (Cook et al. 1967, Dolný et al. 2013). Given that emigration is allowed within these models of open populations, it should be noted that the survival parameters are more accurately considered as "residency" probabilities, i.e. the probability that any individual will remain in the population between sampling occasions, and therefore the longevity estimate is better interpreted as a measure of average residence time.

Description of molecular methods

To establish the diet of the focal species, we used a proven metabarcoding protocol for dragonflies building on our earlier tests for an optimal approach (Kaunisto et al. 2017). In brief, total DNA was extracted from 185 faecal samples in clean 2.0 or 1.5 ml Eppendorf tubes following a salt-extraction protocol (based on Aljanabi and Martinez 1997, and modified by Kaunisto et al. 2017). All the extraction batches included negative controls to account for contamination issues.

Adopting the methods developed during a previous pilot study (Kaunisto et al. 2017), we applied widely utilized Zeale primers: ZBJ-ArtF1c and ZBJ-ArtR2c (hereafter COI; Zeale et al. 2011) to amplify COI region and Clarke primers: Ins16S-1F and Ins16S-1Rshort (hereafter 16S; Clarke et al. 2014) to amplify the 16S region. As these are the most widely used mitochondrial markers for molecular identification of animals, they allow us to compare our results to previous

dietary analyses. As these primers also amplify odonate mtDNA, we designed two blocking primers to decrease predator amplification in favour of the prey amplification (Vestheim and Jarman 2008). For COI we used the Odo-Blk-COI-R 5'-TAC CAA ATC CTC CAA TTA TAA TAG GTA TT-C3 spacer and for 16S we used the Coe-Blk2-R (5'-CCC TAA GGT AAC TTA GTC TAT TGA TCA ATA GTA A-C3 spacer).

Minor modifications were made to the PCR and library preparations: (i) blocking primers were used in 20X concentration compared to primers, (ii) we used MyTaq HS Red Mix (Bioline, UK) as polymerase and (iii) all the PCR reactions were prepared and indexed as duplicates (total reactions: 756 = 185 samples x 2 loci x 2 replicates + 16 negative controls).

The second-step PCR to attach indexed adapters was implemented as in Vesterinen *et al.* (2016), with minor modifications as follows: (a) for a reaction volume of 11.8 µl, we mixed 5.90 µl MyTaq HS Red Mix (Bioline, UK), 0.3 µM forward primer, 0.3 µM reverse primer and 2.40 µl purified locus-specific PCR product (from the first PCR), (b) after indexing, 2 µl of each indexed sample were pooled in four separate subset pools (two COI and two 16S pools) to maximize the diversity of the input template and to allow for scaling the input for each loci/replicate. These pools were purified using dual-SPRI method by Vesterinen *et al.* (2016) as follows: in the first step we added 80 µl (0.8x ratio) SPRI bead solution and in second step 15 µl (0.95x ratio) SPRI bead solution, as we tested that it improves the quality of libraries. All purified subsets pools were combined in equimolar ratios. Sequencing was performed on the Illumina MiSeq platform (Illumina Inc., San Diego, California, USA) by the Turku Centre for Biotechnology, Turku, Finland using v2 chemistry with 300 cycles and 2*150 bp paired-end read length.

Bioinformatics

The sequencing run yielded 16,188,489 quality-controlled paired-end reads. The reads separated by each original sample were uploaded to CSC servers (IT Center for Science, www.csc.fi) for trimming and further analysis. The raw COI dataset encompassed 3,151,809 and the 16S dataset 6,376,734 reads. The rest of the raw reads (n=6,659,946) were either from the PhiX control library or could not be assigned to any sample with perfect dual-index match. Trimming and quality control of the sequences were carried out as follows.

Paired-end reads were merged and trimmed for quality using 32-bit *usearch* version 11 (Edgar 2010) with the command '*fastq_mergepairs*'. Primers were removed using software *cutadapt* version 1.14 (Martin 2011) with 15% mismatch rate. The reads were then collapsed into unique sequences (singletons removed) with command '*fastx_uniques*', denoised (=chimeras were

removed) and reads were clustered into ZOTUs ("ZOTU" = ‘zero-radius OTU’) with command ‘*unoise3*’ using USEARCH version 11. These ZOTUs do not practically differ from traditional clustering of OTUs (which are based on pre-set percentage threshold), but the UNOISE algorithm performs better in (i) removing chimeras, (ii) PhiX sequences and (iii) Illumina artefacts according to Edgar and Flyvbjerg (2015). Then ZOTUs were mapped back to the original trimmed reads with command ‘*search_exact*’ to establish the total number of reads in each sample using 64-bit software *vsearch* (Rognes et al. 2016). We were able to map 3,392,647 reads (COI: 596,062; 16S: 2,796,585) to our original samples. These reads were subject to further filtering: from each sample, we discarded those ZOTUs 1) where only one of the replicate PCR’s produced reads, 2) which had fewer reads assigned to the sample than in any of the multiple (extraction or PCR) negative controls samples, 3) which were present in the data with fewer than 4 reads (for 16S) or 10 reads (COI). This cautious trimming resulted in approximately the same amount of reads for each locus, 449,573 (COI) and 478,202 (16S) filtered reads, which were assigned to prey genera separately for each locus as explained below.

Prey taxa

The prey identification criteria vary for different loci, and thus the prey assignation was done independently for COI and 16S. The COI ZOTUs were initially identified to genus-level using the RDP classifier with a recently constructed COI-RDP database v3.2 (with 60% probability threshold for genus-level assignation) following Porter and Hajibabaei (2018). In cases where the database was clearly insufficient to reach a genus-level assignation, we used local BLAST against all the retrieved COI sequences in BOLD (Altschul et al. 1990, Ratnasingham and Hebert 2007). Finally, the genus name was retrieved manually from BOLD using BIN code or ZOTU sequence, if the information was not otherwise available. The 16S reads were identified to the family-level using command line BLAST against all the sequences in GenBank. Since some BLAST implementations have recently been associated with unintuitive outcomes (see for example Shah et al. 2018 and references therein), we set no limitations on the identifications retrieved. Then, we built a custom script to retrieve the higher taxonomy for each hit, and set the identification threshold to 90% match at the prey genus level.

Roughly half of the filtered COI reads (>49.9%) could be identified to genus level target prey. For filtered 16S reads, ~30% were identified as target prey. This result should be considered good when amplifying arthropod prey DNA mixed with arthropod predator DNA (see for example Piñol *et al.* (2014), where only 6% of reads were assigned to prey in a study without blocking primers). The rest of the reads were either identified to higher taxa only, or were assigned to a

predator damselflies or non-target (such as human) DNA. After assigning each ZOTU to prey genus, we combined locus-specific information and scored the diet at the level of the prey genus. In this study, the most common prey order was Diptera, and the most abundant prey family was Chrinomidae. This pattern was equal for all the odonate species, except *C. hastulatum*, which consumed Sciaridae (Diptera) in higher proportion than Chironomidae.

Additional species- and sex-specific dietary analysis

In a proof-of-concept study, Kaunisto et al. (2017) used prey frequencies instead of prey read abundance. However, as recently indicated, a reliance on presence-absence data may be more misleading than using read abundances (Deagle et al. 2019). Thus, in the present study we adopted a new metric of prey abundance: the relative read abundances (RRA) calculated for each prey taxon in each sample following Vesterinen et al. (2018). Using the sequence counts, relative read abundance (RRA_i) for food item *i* is calculated as (from Deagle et al. 2019):

$$RRA_i = \frac{1}{S}\sum_{k=1}^{S}\frac{n_{i,k}}{\sum_{i=1}^{T} n_{i,k}} \times 100\% \qquad \text{(Eqn S1)}$$

where *T* is the number of food items (taxa), *S* is the number of samples, and $n_{i,k}$ is the number of sequences of food item *i* in sample *k*.

To visualize the trophic interactions structures resolved by the molecular data, we used package "bipartite" (Dormann et al. 2008, 2009) implemented in program R (R Core Team 2018). Quantitative webs were constructed for each odonate predator species and sex, using relative read abundances as explained above. To further explore prey sharing between the four odonate species, we used R package 'VennDiagram' version 1.6.20 (Chen and Boutros 2011) to generate a Venn diagram of overlap in resource use.

Across damselfly species, this yields the following species-specific estimates for the four damselfly species:

C. lunulatum: P_i=(33.9 mg × 0.14 × 7686 x 2.07)= 75 603 mg (Eqn S2a)

C. hastulatum: P_i=(33.9 mg × 0.14 × 5960 x 2.68)= 75 775 mg (Eqn S2b)

C. pulchellum: P_i=(36.1 mg × 0.14 × 6210 x 3.75)= 117 685 mg (Eqn S2c)

E. cyathigerum: P_i=(35.4 mg × 0.14 × 22540 x 4.68)= 523 206 mg (Eqn S2d)

Across all species, this sums to 792,270 mg.

Additional results

Estimates and temporal patterns of damselfly population sizes varied widely across the four species of interest (Figure S1). The sex- and predator-specific food web indicated strong resource sharing between both sexes and all species (Fig. S2). Principal component analysis showed no visible clustering among the samples (Figure S3).

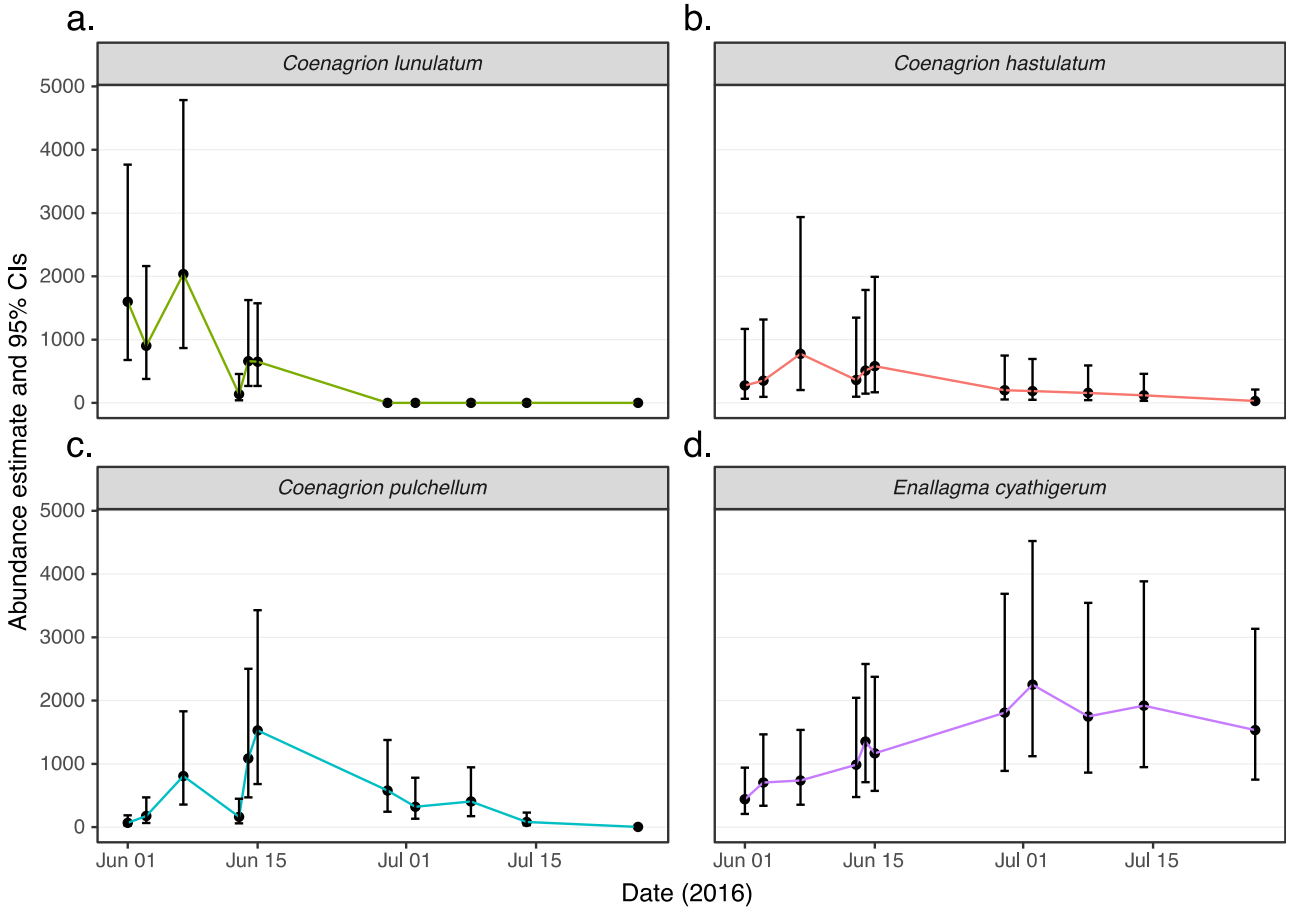

Figure S2. Population estimates across sampling dates derived from best-fitting Jolly-Seber models (POPAN parameterization) for each damselfly species, based on capture-mark-recapture data and processed using program MARK software: a) *Coenagrion lunulatum*, b) *C. hastulatum*, c) *C. pulchellum*, and d) *Enallagama cyathigerum*. Error bars indicate 95% confidence intervals.

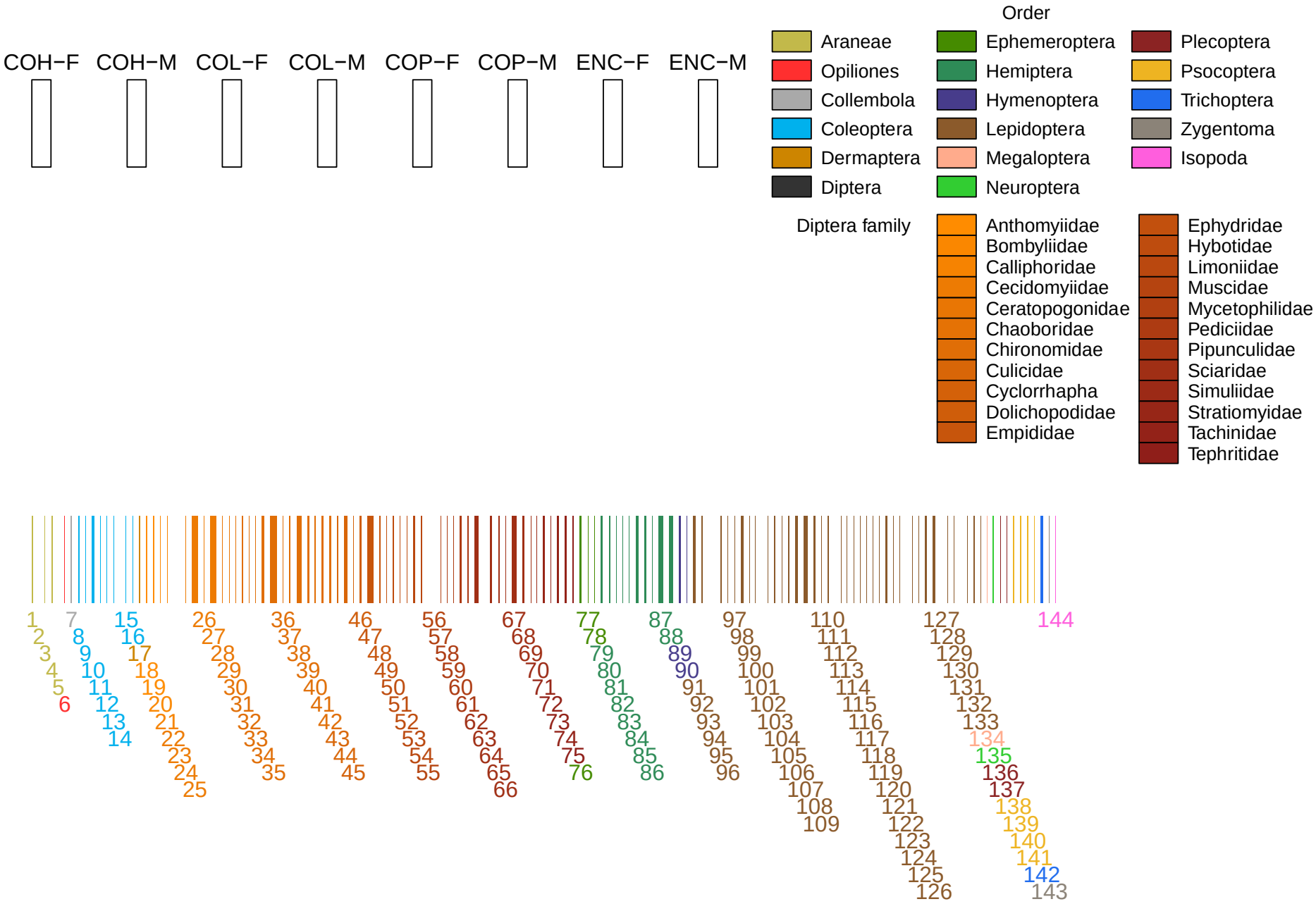
COH−F
COH−M
COL−F
COL−M
COP−F
COP−M
ENC−F
ENC−M
Order
Araneae
Opiliones
Collembola
Coleoptera
Dermaptera
Diptera
Ephemeroptera
Hemiptera
Hymenoptera
Lepidoptera
Megaloptera
Neuroptera
Plecoptera
Psocoptera
Trichoptera
Zygentoma
Isopoda
Diptera family
Anthomyiidae
Bombyliidae
Calliphoridae
Cecidomyiidae
Ceratopogonidae
Chaoboridae
Chironomidae
Culicidae
Cyclorrhapha
Dolichopodidae
Empididae
Ephydridae
Hybotidae
Limoniidae
Muscidae
Mycetophilidae
Pediciidae
Pipunculidae
Sciaridae
Simuliidae
Stratiomyidae
Tachinidae
Tephritidae

Figure S3. Visual representation of the taxonomic distribution and quantified strength of trophic links as resolved by both odonate species and sex. The blocks in the upper row represent predators (COH=*Coenagrion hastulatum*, COL=*C. lunulatum*, COP=*C. pulchellum*, and ENC=*Enallagma cyathigerum;* F=female, M=male). The blocks in the lower row represent prey genera. A line connecting a predator with a prey represents detected predation events, and the thickness of the line represents the relative read abundance (RRA) of each predation record (Eqn S1). See the "Data analysis" in the main text and "Additional species- and sex-specific dietary analysis" above for details on the RRA. The numbers below the lower blocks correspond to the prey family numbers (Table S3).

Table S4. Prey families identified in this study. The first column refers to the family numbers in the plotweb (Figure 1 in the main document). The four columns on the right shows the detailed, proportional (%) prey use by each individual odonate species: *Coenagrion lunulatum* (CL),. *C. hastulatum* (CH), *C. pulchellum* (CP), and *Enallagma cyathigerum* (EC). These proportions (%) are calculated from normalized read abundances as an average across all samples per each odonate as follows: the sequence count for prey item *i* are divided by total sequence count in sample *k* so that sum of all prey item proportions in the sample *k* is 1, then the prey item proportions are summed and divided by the number of samples.

ID	Order	Family	Genus	COH	COL	COP	ENC
	Arachnida						
1	Araneae	Linyphiidae	Bolyphantes	0.00 %	0.00 %	2.76 %	0.00 %
2	Araneae	Linyphiidae	Neriene	0.07 %	0.00 %	0.00 %	0.00 %
3	Araneae	Linyphiidae	Porrhomma	0.00 %	0.66 %	0.00 %	0.00 %
4	Araneae	Linyphiidae	Tenuiphantes	0.00 %	0.00 %	3.31 %	0.00 %
5	Araneae	Theridiidae	Paidiscura	0.00 %	0.01 %	0.00 %	0.00 %
6	Opiliones	Phalangiidae	Mitopus	0.37 %	0.00 %	0.00 %	0.00 %
	Collembola						
7	Collembola	Isotomidae	Isotomidae	2.78 %	0.00 %	0.00 %	0.00 %
	INSECTA						
8	Coleoptera	Brachyceridae	Tanysphyrus	2.58 %	0.00 %	0.00 %	0.00 %
9	Coleoptera	Carabidae	Carabidae	0.00 %	1.30 %	0.00 %	0.00 %
10	Coleoptera	Cerambycidae	Monochamus	0.00 %	2.63 %	0.00 %	3.23 %
11	Coleoptera	Coccinellidae	Adalia	0.17 %	1.10 %	0.00 %	0.00 %
12	Coleoptera	Dytiscidae	Hydaticus	1.39 %	0.00 %	0.00 %	0.00 %
13	Coleoptera	Latridiidae	Cartodere	0.00 %	1.25 %	0.00 %	0.00 %
14	Coleoptera	Scarabaeidae	Eriesthis	0.00 %	0.01 %	0.00 %	0.00 %
15	Coleoptera	Scarabaeidae	Phyllopertha	0.00 %	1.54 %	0.00 %	0.00 %
16	Coleoptera	Staphylinidae	Staphylinidae	0.00 %	0.88 %	0.00 %	0.00 %
17	Dermaptera	Forficulidae	Forficulidae	0.10 %	2.63 %	0.00 %	0.00 %
18	Diptera	Anthomyiidae	Alliopsis	0.00 %	0.00 %	0.00 %	2.02 %
19	Diptera	Anthomyiidae	Paregle	2.75 %	0.00 %	0.00 %	0.00 %
20	Diptera	Bombyliidae	Aldrichina	1.39 %	0.00 %	0.00 %	0.00 %
21	Diptera	Calliphoridae	Calliphora	1.39 %	0.00 %	0.00 %	0.00 %
22	Diptera	Cecidomyiidae	CecidInt12	0.00 %	0.07 %	0.00 %	0.00 %
23	Diptera	Cecidomyiidae	CecidInt26	0.00 %	0.00 %	0.01 %	0.00 %
24	Diptera	Cecidomyiidae	CecidInt3	0.00 %	0.00 %	0.00 %	0.85 %
25	Diptera	Cecidomyiidae	Cecidomyiidae	3.97 %	2.16 %	2.58 %	7.02 %
26	Diptera	Cecidomyiidae	Feltiella	0.00 %	1.26 %	0.00 %	0.00 %
27	Diptera	Cecidomyiidae	Cecidomyiidae	3.97 %	2.16 %	2.58 %	7.02 %
28	Diptera	Ceratopogonidae	Ceratopogonidae	1.20 %	0.00 %	0.00 %	0.00 %
29	Diptera	Ceratopogonidae	Forcipomyia	0.00 %	0.00 %	0.49 %	0.00 %

30	Diptera	Chaoboridae	Chaoborus	0.00 %	1.49 %	0.01 %	0.00 %
31	Diptera	Chironomidae	Chironomus	0.66 %	1.32 %	0.97 %	0.00 %
32	Diptera	Chironomidae	Corynoneura	0.62 %	0.00 %	0.00 %	1.01 %
33	Diptera	Chironomidae	Dicranomyia	0.51 %	0.00 %	0.00 %	0.00 %
34	Diptera	Chironomidae	Glyptotendipes	1.33 %	0.68 %	4.70 %	0.00 %
35	Diptera	Chironomidae	Limnophyes	1.39 %	1.32 %	2.79 %	13.45 %
36	Diptera	Chironomidae	Orthocladiinae	0.00 %	0.15 %	0.00 %	0.00 %
37	Diptera	Chironomidae	Polypedilum	2.78 %	0.00 %	0.00 %	0.00 %
38	Diptera	Chironomidae	Procladius	1.03 %	7.12 %	0.00 %	4.24 %
39	Diptera	Chironomidae	Psectrocladius	0.00 %	0.94 %	3.23 %	0.61 %
40	Diptera	Chironomidae	Pseudorthocladius	0.00 %	0.00 %	0.00 %	2.86 %
41	Diptera	Chironomidae	Smittia	0.00 %	0.00 %	0.00 %	3.03 %
42	Diptera	Chironomidae	Synendotendipes	0.03 %	0.00 %	3.23 %	0.00 %
43	Diptera	Culicidae	Aedes	0.00 %	0.05 %	0.00 %	1.65 %
44	Diptera	Culicidae	Culex	2.78 %	2.63 %	4.13 %	0.00 %
45	Diptera	Cyclorrhapha	Trypetoptera	0.00 %	1.30 %	0.00 %	0.00 %
46	Diptera	Dolichopodidae	Neurigona	1.25 %	2.63 %	0.00 %	0.00 %
47	Diptera	Empididae	Empis	1.75 %	13.51 %	0.00 %	0.00 %
48	Diptera	Empididae	Rhamphomyia	0.19 %	0.00 %	1.51 %	0.00 %
49	Diptera	Ephydridae	Hyadina	0.69 %	0.00 %	0.00 %	0.00 %
50	Diptera	Hybotidae	Euthyneura	1.44 %	0.09 %	1.84 %	0.15 %
51	Diptera	Hybotidae	Leptopeza	1.39 %	0.00 %	0.00 %	0.00 %
52	Diptera	Hybotidae	Trichina	1.39 %	0.00 %	0.00 %	0.00 %
53	Diptera	Limoniidae	Antocha	0.00 %	0.00 %	5.58 %	0.00 %
54	Diptera	Limoniidae	Metalimnobia	0.00 %	0.00 %	0.56 %	1.90 %
55	Diptera	Muscidae	Coenosia	0.00 %	0.00 %	0.00 %	0.07 %
56	Diptera	Muscidae	Hydrotaea	0.00 %	0.00 %	0.02 %	0.00 %
57	Diptera	Mycetophilidae	Mycetophila	0.00 %	1.32 %	0.00 %	0.00 %
58	Diptera	Pediciidae	Pedicia	1.39 %	0.00 %	0.00 %	0.00 %
59	Diptera	Pediciidae	Tricyphona	0.00 %	1.25 %	0.00 %	0.00 %
60	Diptera	Pediciidae	Ula	0.00 %	0.00 %	0.00 %	3.03 %
61	Diptera	Pipunculidae	Cephalops	1.70 %	0.00 %	0.00 %	0.00 %
62	Diptera	Sciaridae	Bradysia	2.86 %	5.41 %	0.00 %	1.52 %
63	Diptera	Sciaridae	Corynoptera	0.00 %	0.00 %	0.00 %	0.02 %
64	Diptera	Sciaridae	Cratyna	3.47 %	0.00 %	0.00 %	0.00 %
65	Diptera	Sciaridae	Ctenosciara	4.06 %	0.00 %	0.00 %	0.00 %
66	Diptera	Sciaridae	Leptosciarella	0.00 %	0.00 %	1.08 %	0.00 %
67	Diptera	Sciaridae	Lycoriella	6.39 %	0.00 %	0.00 %	5.38 %
68	Diptera	Sciaridae	Scatopsciara	1.39 %	0.00 %	3.23 %	0.00 %
69	Diptera	Sciaridae	Xylosciara	0.28 %	0.00 %	0.00 %	0.71 %
70	Diptera	Simuliidae	Simulium	0.00 %	0.00 %	0.15 %	0.00 %
71	Diptera	Stratiomyidae	Microchrysa	4.17 %	0.00 %	0.00 %	0.00 %
72	Diptera	Tachinidae	Chrysoexorista	0.00 %	0.00 %	0.47 %	0.00 %

73	Diptera	Tachinidae	Peleteria	0.00 %	0.00 %	3.23 %	0.00 %
74	Diptera	Tachinidae	Phorocera	0.00 %	1.32 %	0.00 %	3.35 %
75	Diptera	Tephritidae	Dioxyna	0.00 %	0.00 %	3.35 %	0.00 %
76	Ephemeroptera	Baetidae	Cloeon	0.00 %	2.63 %	3.23 %	0.00 %
77	Ephemeroptera	Ephemeridae	Ephemera	0.00 %	0.00 %	1.61 %	0.00 %
78	Ephemeroptera	Heptageniidae	Rhithrogena	1.09 %	0.00 %	0.00 %	0.00 %
79	Hemiptera	Aphididae	Aphis	0.13 %	0.42 %	2.86 %	0.00 %
80	Hemiptera	Aphididae	Euceraphis	0.00 %	0.12 %	0.00 %	4.23 %
81	Hemiptera	Aphididae	Hyalopterus	0.00 %	0.29 %	0.00 %	0.00 %
82	Hemiptera	Cicadidae	Yezoterpnosia	1.39 %	0.00 %	0.00 %	0.00 %
83	Hemiptera	Delphacidae	Javesella	1.66 %	0.00 %	0.00 %	0.00 %
84	Hemiptera	Miridae	Lygus	0.00 %	0.06 %	4.82 %	1.63 %
85	Hemiptera	Miridae	Placochilus	1.42 %	2.06 %	1.61 %	0.00 %
86	Hemiptera	Miridae	Psallus	0.00 %	1.32 %	0.00 %	0.00 %
87	Hemiptera	Psyllidae	Cacopsylla	0.79 %	10.35 %	0.74 %	0.00 %
88	Hemiptera	Psyllidae	Psyllidae	0.00 %	3.82 %	0.37 %	6.06 %
89	Hymenoptera	Cimbicidae	Trichiosoma	0.00 %	0.00 %	3.23 %	0.00 %
90	Hymenoptera	Ichneumonidae	Eusterinx	0.08 %	0.00 %	0.00 %	0.00 %
91	Lepidoptera	Bombycidae	Bombyx	2.83 %	1.16 %	2.20 %	0.00 %
92	Lepidoptera	Coleophoridae	Coleophora	0.00 %	0.00 %	0.00 %	1.77 %
93	Lepidoptera	Crambidae	Palpita	0.00 %	0.00 %	0.00 %	0.15 %
94	Lepidoptera	Erebidae	Arctiinae	0.00 %	0.00 %	0.02 %	0.00 %
95	Lepidoptera	Erebidae	Catocala	0.00 %	0.00 %	0.00 %	3.03 %
96	Lepidoptera	Erebidae	Dasychira	0.00 %	0.00 %	0.00 %	1.36 %
97	Lepidoptera	Erebidae	Lymantria	0.00 %	0.00 %	0.00 %	0.75 %
98	Lepidoptera	Erebidae	Macrochilo	5.56 %	1.08 %	0.00 %	0.00 %
99	Lepidoptera	Erebidae	Naarda	0.00 %	0.00 %	0.11 %	0.00 %
100	Lepidoptera	Gelechiidae	Gelechia	0.00 %	0.00 %	0.63 %	0.00 %
101	Lepidoptera	Gelechiidae	Telphusa	0.00 %	0.00 %	0.00 %	0.02 %
102	Lepidoptera	Geometridae	Hypomecis	0.00 %	0.00 %	0.00 %	1.20 %
103	Lepidoptera	Geometridae	Protoboarmia	0.00 %	0.04 %	0.00 %	3.03 %
104	Lepidoptera	Geometridae	Scopula	0.00 %	0.00 %	0.50 %	0.00 %
105	Lepidoptera	Glyphipterigidae	Glyphipterix	2.65 %	0.00 %	0.00 %	0.00 %
106	Lepidoptera	Gracillariidae	Phyllonorycter	0.00 %	0.00 %	2.72 %	3.03 %
107	Lepidoptera	Heteroneura	Saturnia	8.80 %	0.00 %	1.28 %	0.00 %
108	Lepidoptera	Lasiocampidae	Euthrix	0.00 %	0.00 %	3.23 %	0.00 %
109	Lepidoptera	Lepidoptera	Lepidoptera	0.00 %	0.00 %	0.00 %	0.03 %
110	Lepidoptera	Limacodidae	Apoda	0.00 %	0.00 %	2.87 %	0.00 %
111	Lepidoptera	Noctuidae	Apamea	0.00 %	0.13 %	0.00 %	0.00 %
112	Lepidoptera	Noctuidae	Autographa	0.00 %	0.00 %	0.11 %	0.00 %
113	Lepidoptera	Noctuidae	Axylia	0.00 %	0.00 %	0.24 %	0.00 %
114	Lepidoptera	Noctuidae	Buakea	0.00 %	1.32 %	0.00 %	0.00 %
115	Lepidoptera	Noctuidae	Cosmia	0.00 %	0.00 %	0.43 %	0.00 %

116	Lepidoptera	Noctuidae	Hyalobole	0.00 %	0.00 %	0.47 %	0.00 %
117	Lepidoptera	Noctuidae	Hydraecia	0.00 %	0.00 %	1.75 %	0.02 %
118	Lepidoptera	Noctuidae	Litholomia	0.00 %	0.00 %	0.76 %	0.18 %
119	Lepidoptera	Noctuidae	Noctuidae	0.00 %	0.00 %	3.23 %	0.00 %
120	Lepidoptera	Noctuidae	Parastichtis	0.00 %	0.00 %	0.34 %	0.00 %
121	Lepidoptera	Noctuidae	Spodoptera	0.00 %	0.00 %	0.00 %	1.15 %
122	Lepidoptera	Oecophoridae	Tortricopsis	0.00 %	0.00 %	0.19 %	0.00 %
123	Lepidoptera	Pterophoridae	Gillmeria	0.00 %	0.73 %	0.00 %	0.00 %
124	Lepidoptera	Sphingidae	Mimas	0.00 %	0.00 %	0.00 %	0.33 %
125	Lepidoptera	Tortricidae	Archips	0.00 %	0.00 %	3.23 %	0.19 %
126	Lepidoptera	Tortricidae	Choristoneura	0.00 %	0.00 %	2.61 %	3.11 %
127	Lepidoptera	Tortricidae	Clepsis	0.00 %	0.05 %	0.00 %	0.00 %
128	Lepidoptera	Tortricidae	Epinotia	0.00 %	0.00 %	0.00 %	1.01 %
129	Lepidoptera	Tortricidae	Grapholita	0.00 %	1.34 %	0.00 %	0.00 %
130	Lepidoptera	Tortricidae	Olethreutes	0.00 %	0.00 %	0.18 %	0.00 %
131	Lepidoptera	Tortricidae	Spilonota	0.00 %	0.00 %	0.00 %	1.13 %
132	Lepidoptera	Tortricidae	Tortricidae	0.00 %	0.00 %	0.00 %	3.03 %
133	Lepidoptera	Zygaenidae	Procridinae	0.00 %	0.00 %	0.00 %	0.44 %
134	Megaloptera	Sialidae	Sialis	0.00 %	0.56 %	0.00 %	0.00 %
135	Neuroptera	Chrysopidae	Chrysoperla	2.78 %	0.00 %	0.00 %	0.00 %
136	Plecoptera	Nemouridae	Nemoura	0.00 %	1.32 %	0.00 %	0.00 %
137	Plecoptera	Perlidae	Calineuria	0.25 %	0.00 %	0.00 %	0.00 %
138	Psocoptera	Caeciliusidae	Valenzuela	1.39 %	0.00 %	2.14 %	0.00 %
139	Psocoptera	Lachesillidae	Lachesilla	0.00 %	2.61 %	0.00 %	0.00 %
140	Psocoptera	Psocidae	Psococerastis	2.10 %	0.00 %	0.00 %	0.00 %
141	Psocoptera	Psocidae	Trichadenotecnum	0.00 %	0.20 %	0.00 %	0.00 %
142	Trichoptera	Leptoceridae	Triaenodes	0.00 %	7.59 %	0.00 %	0.00 %
143	Zygentoma	Lepismatidae	Lepisma	0.03 %	0.65 %	0.00 %	0.00 %
	MALACOSTRACA						
144	Isopoda	Asellidae	Asellus	0.00 %	0.00 %	0.51 %	0.00 %

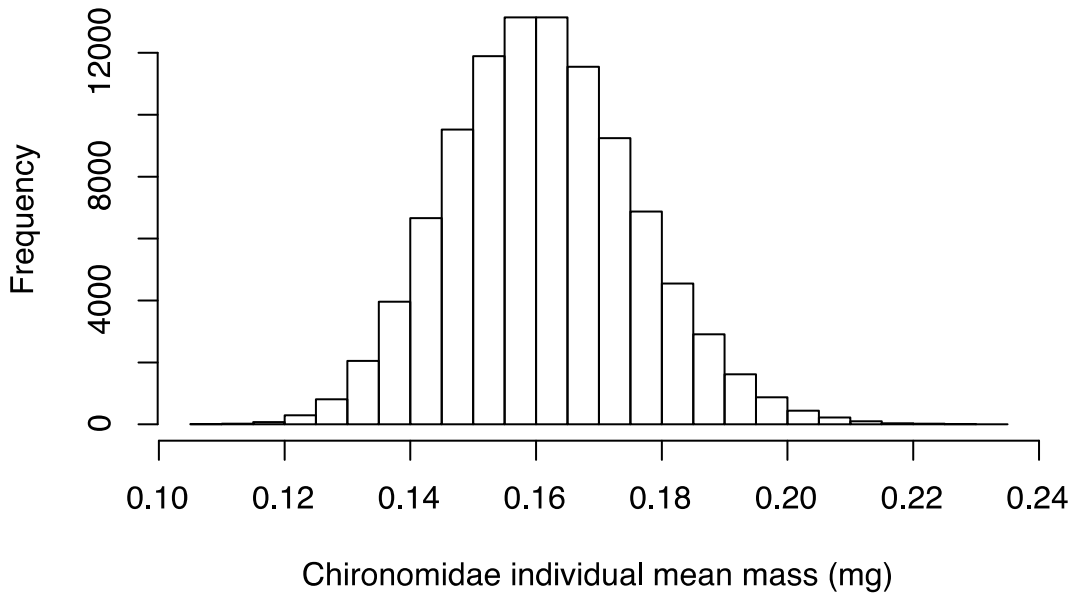

Figure S5. The distribution of individual prey chironomid masses. The original mass data was resampled by bootstrapping 100,000 times. Mean prey individual chironomid mass is 0.16mg (95% CL 0.13–0.19).

References

Aljanabi, S., and I. Martinez. 1997. Universal and rapid salt-extraction of high quality genomic DNA for PCR- based techniques. Nucleic Acids Research 25:4692–4693.

Altschul, S. F., W. Gish, W. Miller, E. W. Myers, and D. J. Lipman. 1990. Basic local alignment search tool. Journal of molecular biology 215:403–410.

Burnham, K. P., and D. R. Anderson. 2002. Model selection and multi-model inference: a practical information theoretical approach. Second edition. Springer, Berlin.

Chen, H., and P. C. Boutros. 2011. VennDiagram: a package for the generation of highly-customizable Venn and Euler diagrams in R. BMC Bioinformatics 12.

Clarke, L. J., J. Soubrier, L. S. Weyrich, and A. Cooper. 2014. Environmental metabarcodes for insects: *in silico* PCR reveals potential for taxonomic bias. Molecular Ecology Resources 14:1160–1170.

Cooch, E., and G. White. 2018. Program MARK: A gentle introduction. 18th edition.

Cook, L. M., L. P. Brower, and H. J. Croze. 1967. The accuracy of a population estimation from multiple recapture data. The Journal of Animal Ecology:57–60.

Deagle, B. E., A. C. Thomas, J. C. McInnes, L. J. Clarke, E. J. Vesterinen, E. L. Clare, T. R. Kartzinel, and J. P. Eveson. 2019. Counting with DNA in metabarcoding studies: How should we convert sequence reads to dietary data? Molecular Ecology 28:391–406.

Dolný, A., H. Mižičová, and F. Harabiš. 2013. Natal philopatry in four European species of dragonflies (Odonata: Sympetrinae) and possible implications for conservation management. Journal of insect conservation 17:821–829.

Dormann, C. F., J. Frund, N. Bluthgen, and B. Gruber. 2009. Indices, Graphs and Null Models: Analyzing Bipartite Ecological Networks. The Open Ecology Journal 2:7–24.

Dormann, C. F., B. Gruber, and J. Fruend. 2008. Introducing the bipartite Package: Analysing Ecological Networks. R News 8:8–11.

Edgar, R. C. 2010. Search and clustering orders of magnitude faster than BLAST. Bioinformatics 26:2460–2461.

Edgar, R. C., and H. Flyvbjerg. 2015. Error filtering, pair assembly and error correction for next-generation sequencing reads. Bioinformatics 31:3476–3482.

Kaunisto, K. M., T. Roslin, I. E. Sääksjärvi, and E. J. Vesterinen. 2017. Pellets of proof: First glimpse of the dietary composition of adult odonates as revealed by metabarcoding of feces. Ecology and Evolution 7:8588–8598.

Lebreton, J.-D., K. P. Burnham, J. Clobert, and D. R. Anderson. 1992. Modeling survival and testing biological hypotheses using marked animals: a unified approach with case studies. Ecological monographs 62:67–118.

Lilley, T., L. Ruokolainen, E. Vesterinen, L. Paasivirta, and K. Norrdahl. 2012. Sediment organic tin contamination promotes impoverishment of non-biting midge species communities in the Archipelago Sea, S-W Finland. Ecotoxicology 21:1333–1344.

Martin, M. 2011. Cutadapt removes adapter sequences from high-throughput sequencing reads. EMBnet.journal 17:10.

Piñol, J., V. San Andrés, E. L. Clare, G. Mir, and W. O. C. Symondson. 2014. A pragmatic approach to the analysis of diets of generalist predators: the use of next-generation sequencing with no blocking probes. Molecular Ecology Resources 14:18–26.

Porter, T. M., and M. Hajibabaei. 2018. Automated high throughput animal CO1 metabarcode classification. Scientific Reports 8.

R Core Team. 2018. R: A Language and Environment for Statistical Computing. R Foundation for Statistical Computing, Vienna, Austria.

Ratnasingham, S., and P. Hebert. 2007. BOLD: The Barcode of Life Data System (www.barcodinglife.org). Molecular Ecology Notes 7:355–364.

Rognes, T., T. Flouri, B. Nichols, C. Quince, and F. Mahé. 2016. VSEARCH: a versatile open source tool for metagenomics. PeerJ 4:e2584.

Shah, N., M. G. Nute, T. Warnow, and M. Pop. 2018. Misunderstood parameter of NCBI BLAST impacts the correctness of bioinformatics workflows. Bioinformatics.

Vesterinen, E. J., A. I. E. Puisto, A. Blomberg, and T. M. Lilley. 2018. Table for five, please: dietary partitioning in boreal bats. Ecology and Evolution 8:10914–10937.

Vesterinen, E. J., L. Ruokolainen, N. Wahlberg, C. Peña, T. Roslin, V. N. Laine, V. Vasko, I. E. Sääksjärvi, K. Norrdahl, and T. M. Lilley. 2016. What you need is what you eat? Prey selection by the bat *Myotis daubentonii*. Molecular Ecology 25:1581–1594.

Vestheim, H., and S. N. Jarman. 2008. Blocking primers to enhance PCR amplification of rare sequences in mixed samples – a case study on prey DNA in Antarctic krill stomachs. Frontiers in Zoology 5:12.

Zeale, M. R. K., R. K. Butlin, G. L. A. Barker, D. C. Lees, and G. Jones. 2011. Taxon-specific PCR for DNA barcoding arthropod prey in bat faeces. Molecular Ecology Resources 11:236–244.